Article

Enhanced Artificial Gorilla Troops Optimizer Based Clustering Protocol for UAV-Assisted Intelligent Vehicular Network

Hadeel Alsolai [1], Jaber S. Alzahrani [2], Mohammed Maray [3], Mohammed Alghamdi [3,4], Ayman Qahmash [3], Mrim M. Alnfiai [5], Amira Sayed A. Aziz [6] and Anwer Mustafa Hilal [7,*]

1   Department of Information Systems, College of Computer and Information Sciences, Princess Nourah bint Abdulrahman University, Riyadh 11671, Saudi Arabia
2   Department of Industrial Engineering, College of Engineering at Alqunfudah, Umm Al-Qura University, Makkah 24382, Saudi Arabia
3   Department of Information Systems, College of Computer Science, King Khalid University, Abha 62529, Saudi Arabia
4   Department of Information and Technology Systems, College of Computer Science and Engineering, University of Jeddah, Jeddah 23218, Saudi Arabia
5   Department of Information Technology, College of Computers and Information Technology, Taif University, Taif 21944, Saudi Arabia
6   Department of Digital Media, Faculty of Computers and Information Technology, Future University in Egypt, New Cairo 11835, Egypt
7   Department of Computer and Self Development, Preparatory Year Deanship, Prince Sattam bin Abdulaziz University, Al-Kharj 16278, Saudi Arabia
*   Correspondence: a.hilal@psau.edu.sa

Abstract: The increasing demands of several emergent services brought new communication problems to vehicular networks (VNs). It is predicted that the transmission system assimilated with unmanned aerial vehicles (UAVs) fulfills the requirement of next-generation vehicular network. Because of its higher flexible mobility, the UAV-aided vehicular network brings transformative and far-reaching benefits with extremely high data rates; considerably improved security and reliability; massive and hyper-fast wireless access; much greener, smarter, and longer 3D communications coverage. The clustering technique in UAV-aided VN is a difficult process because of the limited energy of UAVs, higher mobility, unstable links, and dynamic topology. Therefore, this study introduced an Enhanced Artificial Gorilla Troops Optimizer–based Clustering Protocol for a UAV-Assisted Intelligent Vehicular Network (EAGTOC-UIVN). The goal of the EAGTOC-UIVN technique lies in the clustering of the nodes in UAV-based VN to achieve maximum lifetime and energy efficiency. In the presented EAGTOC-UIVN technique, the EAGTO algorithm was primarily designed by the use of the circle chaotic mapping technique. Moreover, the EAGTOC-UIVN technique computes a fitness function with the inclusion of multiple parameters. To depict the improved performance of the EAGTOC-UIVN technique, a widespread simulation analysis was performed. The comparison study demonstrated the enhancements of the EAGTOC-UIVN technique over other recent approaches.

Keywords: vehicular networks; unmanned aerial vehicles; clustering; gorilla troops optimizer; fitness function

1. Introduction

Transport commuting becomes a ubiquitous part of day to day lives; the vehicular network (VN) plays a positive role and increases the quality of life [1]. VN technology is advantageous in information applications, automatic toll collection, public safety, automatic driving, traffic coordination, event-driven safety message broadcasting, and so on. VN accesses the location where a traffic accident occurs, timely notifies the pertinent vehicle to adopt security measurement, and then offers quality of service of multimedia information for the tourist during the journey. Regarding the data services, VN is applied for the

remainder of services with respect to infectious diseases, carbon emissions, pollution levels of the haze, and other related services that could enhance the living environment of humans [2]. Moreover, traffic-flow coordination could be benefitted by VN. People timely obtain present traffic data on the road of the vehicle and select the optimum path. These data are particularly effective for the best travel experience for the passenger and for preventing congested sections. Intelligent transport systems benefited considerably from VN [3]. It provides data with respect to restaurants, petrol stations, weather information, navigation, service areas, and every desirable datum regarding the neighboring environments. VN is employed to automated driving, namely the distance detection among velocity estimation, vehicles, road-condition perception, self-parking, and location service [4]. VN is employed to realize automated charging of the vehicle. In V2I transmission, RSU could automatically sense the journey mileage of a vehicle, the entrance location, and exit location, later realizing the automated charging that could decrease the congestion at the charging place and enhance the charging efficiency [5]. Figure 1 depicts the framework of UAV-assisted vehicular network.
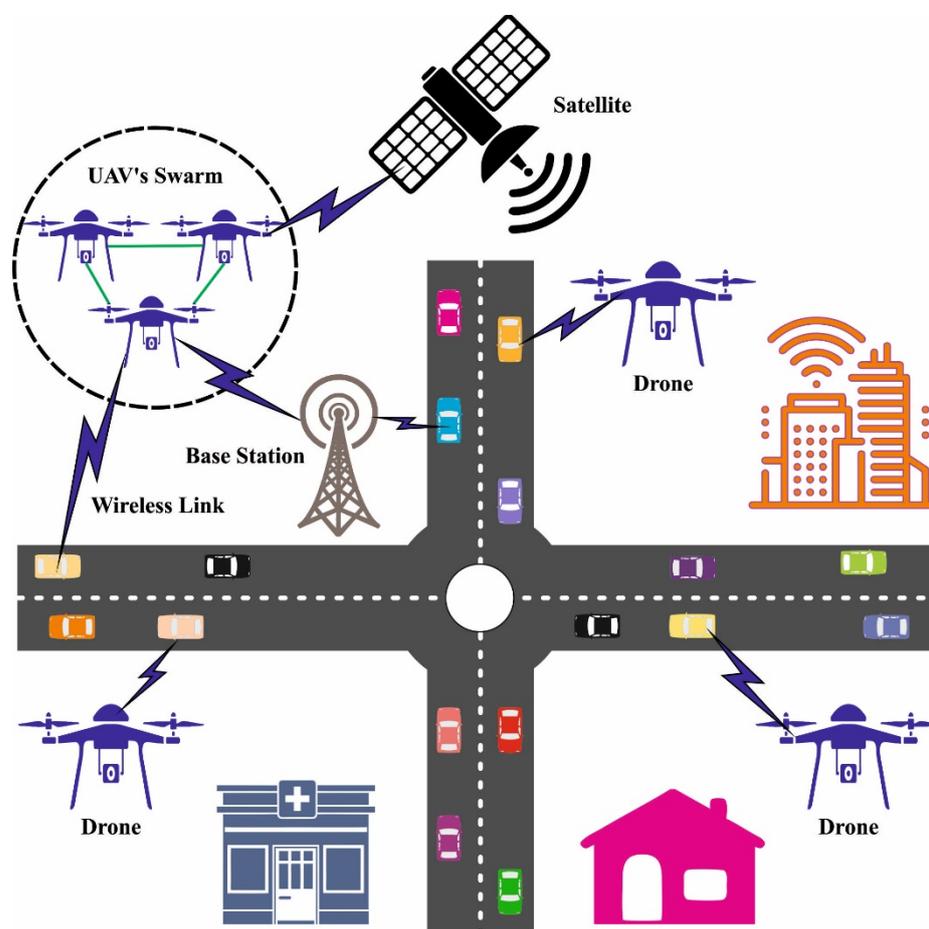

Figure 1. Structure of UAV-assisted vehicular network.

A data-distribution technique is broadly employed in different circumstances, namely emergency collision avoidance [6], the data acquirement of public entertainment, and traffic-flow management that could decrease the number of traffic accidents, which promote the urban building of a smart city and discharge urban traffic congestion [7]. In certain scenarios, the timeliness of data dissemination is crucial. To accomplish the objective, unmanned aerial vehicle (UAV) is applied to help with data distribution. Due to better maneuverability of the UAV, it is widely used for completing the data dissemination task in certain scenarios [8]. For instance, in certain locations, once the transmission framework

is damaged, the UAV could be deployed rapidly as the mobile base station to help the transmission network. Network lifetime is a significant parameter in UAV network that is based on whether a specific number of nodes die due to energy consumption [9]. In mobile UAV networks, topology control is the major aspect for extending network lifetime and reducing communication interference. A hierarchical network based on clustering model is widely employed in mobile networks. The cluster head (CH) selection and clustering process are major factors in the hierarchical network [10–12].

This study introduces an Enhanced Artificial Gorilla Troops Optimizer based Clustering Protocol for UAV-Assisted Intelligent Vehicular Network (EAGTOC-UIVN). The goal of the EAGTOC-UIVN technique lies in the clustering of the nodes in UAV-based VN to achieve maximum lifetime and energy efficiency. In the presented EAGTOC-UIVN technique, the EAGTO algorithm is primarily designed by the use of circle chaotic mapping technique. Moreover, the EAGTOC-UIVN technique computes a fitness function with the inclusion of multiple parameters. To depict the improved performance of the EAGTOC-UIVN technique, a widespread simulation analysis was performed.

2. Literature Review

In Reference [13], an efficient routing technique depending upon a flooding method was developed for robust route identification. It assures an alternate path during path-failure scenarios. In addition, a forecasting approach is employed for anticipating the expiration time of every discovered route. The authors in Reference [14] considered the issue of content distribution to the vehicles on roadways with overloaded or no available communication structure. Incoming vehicles demand service from a library of content which is partially cached at the UAV; the content of the library is also considered for modifying new vehicles carrying more popular content. A non-orthogonal multiple access (NOMA)-enabled double-layer airborne access vehicular ad hoc networks (DLAA-VANETs) architecture was designed in Reference [15], which consists of a high-altitude platform (HAP), multiple unmanned aerial vehicles (UAVs), and vehicles. For the designed DLAA-VANETs, the UAV deployment and network optimization problem is addressed. Particularly, the UAV deployment method, depending upon particle swarm optimization, is presented. Next, the NOMA model is introduced into the designed model for improving the transmission rate.

Khabbaz et al. [16] aimed at enhancing the ground vehicle connectivity in the framework of an alternating vehicle-to-UAV (V2U) transmission condition, whereas vehicles create time-limited connectivity with transient by UAV served as flying BSs responsible to route arriving vehicle information on backbone network or Internet. Zheng et al. [17] used cyclic-flight UAVs for assisting RSU by offering video download services to vehicles. With the utilization of UAV, seamless communication coverage and stable broadcast connections ensure the optimum quality of services to vehicle. Moreover, the authors present a model-free technique dependent upon DQN for determining an optimum UAV decision procedure for achieving the minimization of stalling time. Raza et al. [18] examined a UAV-assisted VANET communication structure, whereas UAVs fly over the used region and offer communication service to basic coverage region. UAV-assisted VANET aims for the benefits of line-of-sight (LOS) communication, flexibility, load balancing (LB), and cost-effectual deployment.

Wu et al. [19] examined a deep supervised learning system to enable intelligence edge for making decisions on the extremely dynamic vehicular network. Specifically, the authors initially presented a clustering-based two-layered (CBTL) technique for solving the JCTO problem offline. Afterward, they planned a deep supervised learning structure of CNN for making fast decisions online. Ghazzai et al. [20] established a mobility- and energy-aware data routing protocol for UAV-supported VANETs. Most UAVs perform as a flying RSU, gathering information in ground vehicles, but another UAV role is the play of relays for providing the information to mobility service center (MSC). The UAV is modifying its 3D places in an existing range if required for ensuring reliable communication links.

A UAV-helped data dissemination system dependent upon network coding was presented in Reference [21]. Initially, the graph concept for modeling the occurrence of data loss of the vehicles was utilized; the data dissemination issue was changed to the maximal clique issue of graphs. With the coverage of directional antenna being restricted, a parallel system for determining the maximal clique dependent upon the area separation was presented. Alioua et al. [22] examine a new distributed SDN-related structure for UAV-support-structure-less vehicular networks. An important purpose is to fill the gap in which no SDN-based infrastructure was presented for these networks. The author's concentrated mostly on a road safety use-case that integrated UAVs for assisting emergency vehicles in the exploration of affected regions from crucial emergency conditions. In addition, the authors examined an effectual data processing strategy with shared decision-making or computation-offloading problems. Though several models are available in the literature, the network efficiency in UAV-assisted VNs still needs to be improved. In addition, the inclusion of multiple parameters for optimal UAV selection is important as CHs become essential.

3. The Proposed Model

In this study, a new EAGTOC-UIVN technique was developed for clustering the UAV-assisted VN. The major aim of the EAGTOC-UIVN technique exists in the grouping of the nodes in the UAV-based VN to achieve maximum lifetime and energy efficiency. In the presented EAGTOC-UIVN technique, the EAGTO algorithm is primarily designed by the use of the circle chaotic mapping technique.

3.1. System Model

In the presented model, the types of UAVs considered could be middle-size drones or mini drones. A simple collision process is utilized for collision avoidance [23]. In this work, the UAV changed altitude for possible collision. The UAV's maximum speed could reach up to 30 m/s. Every UAV device relies on a location-aware component. This location-conscious mechanism allows the routing method to function efficiently and precisely. In general, location data can be attained from an alternative scheme. In the presented method, inertial measurement units and GPS are given for the motion sensing and positioning of the UAV. Each UAV is aware of its ground station and neighbors' positions. Each UAV is equipped with long- and short-range wireless transmission. Long-range wireless transmission can be utilized for inter-cluster transmission with the ground station and other CHs. Short-range wireless transmission is utilized for intra-transmission with its peers in the cluster.

3.2. Design of EAGTO Technique

With other metaheuristics, AGTO's stability and convergence accuracy suffer as the optimization problem to be resolved grows in variety and complexity. This flaw requires the further development of novel mechanisms to perform exploitation and exploration and help accomplish improved performance [24]. A troop comprises a dominant adult male gorilla (silverback), numerous dominant adult females, and their offspring. A silverback gorilla is over 12 years old and obtains the name from the distinct hairs that grow on his back while he attains puberty. Furthermore, the silverback is the leader of the entire troop and is accountable for ensuring everyone's safety, planning and executing group travel, allocating food and other resources, and making each decision, mediating any conflicts that arise. Male gorillas between the ages of 8 and 12 are considered "black" since the silver fur is not fully grown. It is common for gorillas to leave the birth group for joining a third. However, some male gorillas decide to stick around and keep following the silverback. Such males might fight viciously for controlling the group and accessing adult females when the silverback is killed. The idea of group behaviors in wild gorillas acts as the motivation for the AGTO algorithm. Initialization, local exploitation, and global exploration are the three phases that make up AGTO, the same as they are in other intelligent techniques.

3.2.1. Initialization Phase

Consider the *D*-dimension space has *N* gorillas. To specify where *i-th* gorillas are in the universe, we could formulate $X_i = (x_{i,1}, x_{i,2}, \ldots x_{i,D})$, whereas $I = 1, 2, \ldots N$, and it can be defined as follows:

$$X_{N \times D} = rand(N, D) \times (ub - lb) + lb \ (1) \tag{1}$$

where rand () lies between 0 and 1. The search range can be determined by using the upper and lower limits, *ub* and *lb*, respectively; and the matrix, *X*, has a random value, *A*, within [0, 1] that is allocated to all the elements of the *N* rows and *D* columns in the matrix represented as *rand* (*N*, *D*).

3.2.2. Exploration Phase

$$GX(t+1) = (ub - lb) \times r2 + lb, \ r1 < p$$

$$(r3 - C) \times XA(t) + L \times Z \times X(t), \ r1 \geq 0.5$$

$$X(t) - L \times (L \times (X(t) - XB(t)) + r4 \times (X(t) - XB(t)))r1 < 0.5 \tag{2}$$

In the above equations, *t* signifies iteration times, $X(t)$ indicates the gorilla's existing location vector, and $GX(t+1)$ denotes the potential search agent position for the following iteration. Furthermore, the random numbers *r1*, *r2*, *r3*, and *r4* denote a number value between zero and one. Two locations among the existing population of gorillas, $XA(t)$ and $B(t)$, are selected randomly; *p* is a predetermined value. By utilizing the problem dimension as an index, *Z* denotes the row vector where the component value was derived randomly from $[-C, C]$. Additionally, *C* can be defined as follows:

$$C = (\cos(2 \times r5) + 1) \times \left(1 - \frac{t}{Maxiter}\right) \tag{3}$$

where cos (●) denotes the cosine function, r_5 indicates positive real numbers amongst [0, 1], and *Maxiter* denotes the maximal iteration number. It is possible to evaluate *L*, the value of variable, as follows:

$$L = C \times l \tag{4}$$

where *l* indicates the arbitrary value within $[-1, 1]$. Afterward, every probable $GX(t+1)$ solution is produced, owing to the exploration, and the fitness value is compared. If *GX* outperformes *X*, it is kept and utilized in the location of *X*. This is represented as the condition $(GX) < F(X)$, whereas *F* indicates the fitness function for the problem in question (t). Additionally, the better option available at the time is now considered to be the silverback.

3.2.3. Exploitation Phase

Once the new troop of gorillas is formed, the silverback is the dominant male and is at the peak of his health and strength. They follow the silverback gorilla since they forage for food. Unavoidably, the silverback will age and die, and in his location, a younger blackback in the troop might engage in fighting over mating and leadership with other males. AGTO's exploitation stage follows the silverback and competes for adult female gorillas. *W* is presented for controlling these transitions. When *C* in Equation (4) is higher than *W*, this follows the silverback's initial model:

$$GX(t+1) = L \times M \times (X(t) - Xsilverback) + X(t) \tag{5}$$

In such cases, the optimum solution found so far is indicated as X silverback, the existing location vector is represented as (t), and L is estimated by means of Equation (5). The values of M are defined as follows:

$$M = \left(\frac{\sum_{i=1}^{n} xi(t)}{N|\frac{xi(t)}{N}|^{2l}} \right) \frac{1}{2l} \tag{6}$$

where N denotes the overall individual number, and $Xi(t)$ indicates a vector demonstrating the gorilla's position:

$$GX(t+1) = Xsilverback - (Xsilverback \times Q - X(t) \times Q) \times A \tag{7}$$

$$Q = 2 \times r6 - 1 \tag{8}$$

$$A = \phi \times E, \tag{9}$$

$$E = \begin{cases} N1, & r7 \geq 0.5 \\ N2, & r7 < 0.5 \end{cases} \tag{10}$$

It is the existing location, represented as (t), and the impact force, Q, that are evaluated by Equations (7) and (8). A random value within zero and one is utilized for $r6$ in Equation (4). Additionally, Equation (9) is utilized for assessing the efficiency of the coefficient. A is utilized for stimulating the level of violence in the game. With the equation denoting a constant, we could define what number represents Equation (10). Equation (6) involves $r7$, which is a value selected randomly within zero and one. Standard distribution, $E(1, D)$, is when r70.5 is a coincidental event, and D indicates the number of spatial dimensions. However, if $r7$ is less than half, E is equivalent to the random quantity that fits neatly into the standard distribution. Afterward, the exploitation stage is complete, and the value of candidate fitness for the recently generated $GX(t+1)$ problems is calculated. GX is preserved if $F(GX)F$. Figure 2 depicts the flowchart of GTOA.

Figure 2. Flowchart of GTOA.

In this work, the EAGTO algorithm was primarily designed by the use of the circle chaotic mapping technique. To increase the population diversity and exploit the data in the solution space, the circle chaotic function is proposed to increase the initialization mode of the GTOA. Additionally, it can be mathematically expressed as follows:

$$z_{k+1} = z_k + b - \frac{a}{2\pi} \cdot \sin(a\pi z_k) mod(1), z_k \in (0,1) \tag{11}$$

whereas $a = 0.5$ and $b = 0.2$, the circle mapping and random search mechanism are chosen to be independently implemented 300 times. The traversal of circle chaotic mapping is more homogeneously distributed and wider in the range of [0, 1]. Thus, after integrating circle chaotic mapping, the presented technique has a robust global exploration capability.

3.3. Clustering Process Involved in EAGTOC-UIVN Technique

The EAGTOC-UIVN technique computes a fitness function with the inclusion of multiple parameters. The EAGTOC-UIVN method is proposed with the existence of 4 fitness variables, namely energy efficacy of cluster node density, UAV nodes, distance in CH to sink, and average distance of UAV for CH enclosed by their sensing series [25]. The data on fitness parameters was provided by the following:

Energy efficiency: The *CH* executes various events, such as gathered, sense, data broadcast, aggregation, and so on; hence, *CH* intakes the greatest amount of energy when compared to other nodes. Then it is vital for defining an *FF* that shared the load among each UAV from the network. The fitness variable for effective deployment of network energy is given below:

$$R_e = e(n_i)$$

$$Avg_e = \frac{1}{n} \sum_{i=0}^{n} e(n_i)$$

$$f_1 = CH_{opt} * \frac{R_e}{Avg_e} = \frac{CH_{opt} * e(n_i)}{\frac{1}{n}\Sigma_{i=0}^{n} e(n_i)} \forall CH_{opt} = 5\% \ of \ n, \ e(n_i)$$
$$= 0.5J \ or \ 1.25J \ or \ 1.75J \tag{12}$$

In Equation (12), R_e, Avg_e, and n_i denote the node RE, network average energy, and whole quantity of UAV nodes, respectively. CH_{opt} shows the optimum percentage of CHs.

Cluster node density: In intra-cluster communication, the cost is a crucial parameter for the high energy effectiveness of the network. Next, the network energy deployment was larger when the cost function of cluster was determined as follows:

$$f_2 = \max\left(n(CH_1), n(CH_2), n(CH_3) n(CH_j)\right) \forall n = 2 \ To \ 95, \ j = 1 \ to \ 15 \tag{13}$$

From the expression, $n(CH_j)$ denotes the number of UAVs from the range of jth CH (CH_j). The values of objective function f_2 are greater than able choice of *CH* and exploits from reducing the energy reduction.

The average distance of UAVs to the *CH* within its sensing range: In intra-cluster communication, UAVs transmit information to the *CH*. When the *CH* is farther from the CM, the energy of the UAV diminishes; when the *CH* is closer to the member UAV nodes afterward, there is a deployment of minimal energy.

$$f_3 = \frac{1}{n_{s\tau}} \sum_{i=0}^{n_{sr}} disT(CH, i) \ \forall dist(CH, i) = 1 \ to \ 35 \ m, n_{sr} = 1 \ to \ 100 \tag{14}$$

where n_{sr} and $dist(CH, i)$ indicate the number of UAVs from the sensing sequence and Euclidean distance in node and *CH* from the sensing series of the cluster. Thus, the value of f_3 is minimal; however, the intra-cluster communication power is lessened.

Distance from *CH* to *BS*: The distance between the *BS*s and *CH*s takes a basic function, as if the *CHS* is farther from the sink and exploits energy quickly that is evaluated by the following:

$$f_4 = \frac{1}{CH} \sum_{i=0}^{CH} dist(BS, CH_i) \; \forall dist(BS, CH_i) = 1 \; to \; 70m, \; CH = 1 \; to \; 15 \qquad (15)$$

In Equation (15), $dist(BS, CH_i)$ indicates the Euclidean distance among the *BS* and CH_i. Minimizing the f_4 objective function specified that the *CHS* is not farther from the *BS*.

Once the f_1, f_2, f_3, and f_4 function parameters were evaluated, the objective function was also named FF and calculated as follows:

$$F = Maximize \; Fitness = \alpha * f_1 + \beta * f_2 + \gamma * \frac{1}{f_3} + \delta * \frac{1}{f_4} \qquad (16)$$

In Equation (16), α, β, γ, and δ denote the weight coefficient for the f_1, f_2, f_3, and f_4 FF parameters, correspondingly. The range of weight coefficient ranges from 0 to 1.

4. Results and Discussion

The proposed model was simulated by using MATLAB R2019a. The simulation parameters are listed in Table 1. In this section, a detailed experimental validation of the EAGTOC-UIVN approach is investigated under distinct UAVs. Table 2 and Figure 3 report an overall PDR examination of the EAGTOC-UIVN model under several UAVs, with existing models such as swarm-intelligence-based clustering (SIC), EALC, ant-colony optimization (ACO), GBLADSR, and genetic algorithm (GA) [23].

Table 1. Parameter settings.

Parameter	Value
Network area	1000 m*1000 m
UAV transmission range	250–300 m
Number of UAVs	150
Number of ground station	1
Traffic type	CBR
CBR rate	2 Mbps
Speed	10–30 m/s
UAV transmission power	5 W

Table 2. PDR analysis of EAGTOC-UIVN approach with other systems under varying UAVs.

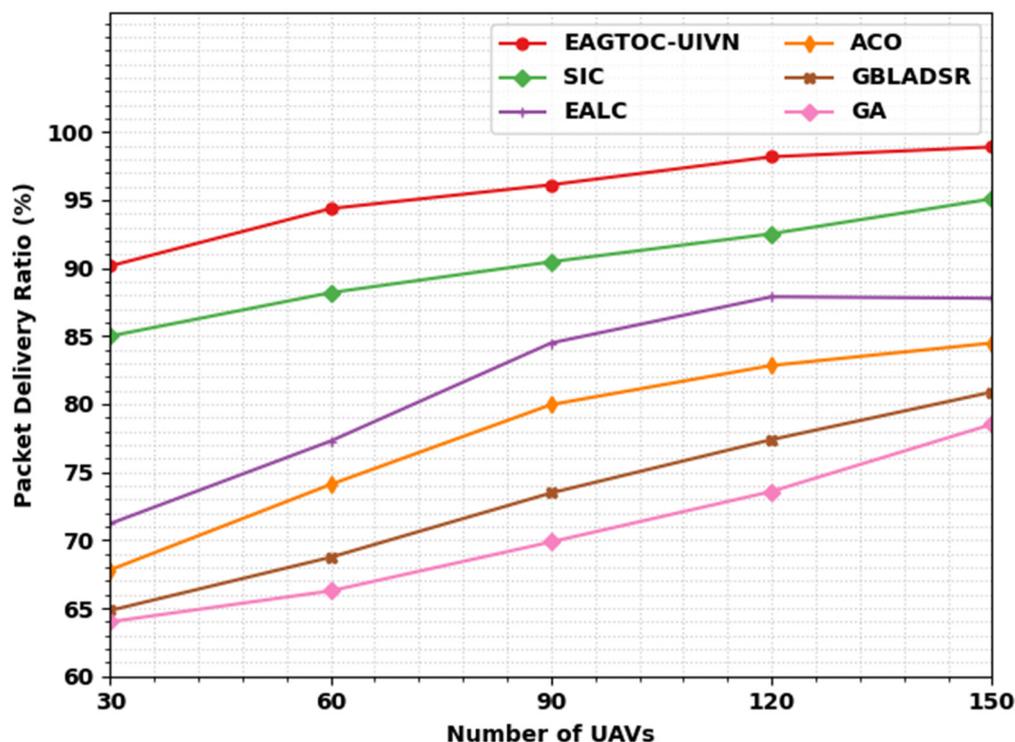| Packet Delivery Ratio (%)					
Number of UAVs	EAGTOC-UIVN	SIC	EALC	ACO	GBLADSR	GA
30	90.15	85.00	71.21	67.81	64.83	64.00
60	94.37	88.19	77.28	74.09	68.74	66.27
90	96.12	90.46	84.49	79.96	73.47	69.87
120	98.18	92.52	87.89	82.84	77.39	73.58
150	98.90	95.09	87.78	84.49	80.89	78.52

Figure 3. PDR analysis of EAGTOC-UIVN system under varying UAVs.

The experimental value implies that the EAGTOC-UIVN technique obtained a better performance under all UAVs. For example, on 30 UAVs, the EAGTOC-UIVN method reached an increased PDR value of 90.15%. On the other hand, the SIC, EALC, ACO, GBLADSR, and GA approaches accomplished decreased PDR values of 85%, 71.21%, 67.81%, 64.83%, and 64%, correspondingly. Meanwhile, on 150 UAVs, the EAGTOC-UIVN technique attained an improved PDR value of 98.90%. In contrast, the SIC, EALC, ACO, GBLADSR, and GA techniques attained reduced PDR values of 95.09%, 87.78%, 84.49%, 80.89%, and 78.52%, correspondingly.

In Table 3 and Figure 4, a brief average end-to-end delay (AETED) assessment of the EAGTOC-UIVN with recent techniques is given. The results implied that the GA model failed to portray effectual outcomes with maximum values of AETED. At the same time, the EALC, ACO, and GBLADSR models reached closer AETED values. Although the SIC model tried to show a reasonable AETED value, the EAGTOC-UIVN model gained effectual outcomes with minimal AETED values. Notice that the EAGTOC-UIVN model reached an AETED value of at least 0.078 s under 30 UAVs.

Table 3. AETED analysis of EAGTOC-UIVN approach with other systems under varying UAVs.

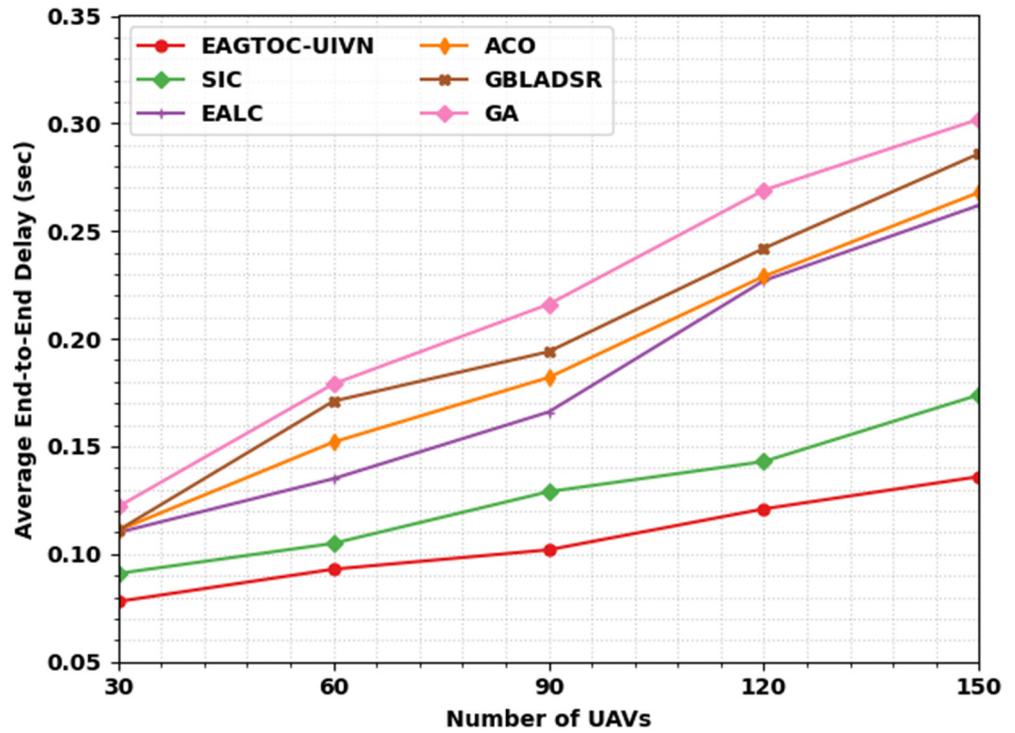| Average End-to-End Delay (s)					
Number of UAVs	EAGTOC-UIVN	SIC	EALC	ACO	GBLADSR	GA
30	0.078	0.091	0.110	0.111	0.111	0.122
60	0.093	0.105	0.135	0.152	0.171	0.179
90	0.102	0.129	0.166	0.182	0.194	0.216
120	0.121	0.143	0.227	0.229	0.242	0.269
150	0.136	0.174	0.262	0.268	0.286	0.302

Figure 4. AETED analysis of EAGTOC-UIVN algorithm under varying UAVs.

In Table 4 and Figure 5, a brief cluster overhead (COH) assessment of the EAGTOC-UIVN with recent techniques is given. The result implies that the GA technique failed to represent effectual outcomes with a maximal value of COH. Simultaneously, the EALC, ACO, and GBLADSR techniques attained closer COH values. Even though the SIC method tried to demonstrate a reasonable COH value, the EAGTOC-UIVN technique obtained effectual outcomes with minimal COH values. Note that the EAGTOC-UIVN methodology attained a minimum COH value of 0.153 under 30 UAVs.

Table 4. COH analysis of EAGTOC-UIVN technique with other systems under varying UAVs.

	Cluster Overhead					
Number of UAVs	**EAGTOC-UIVN**	**SIC**	**EALC**	**ACO**	**GBLADSR**	**GA**
30	0.153	0.160	0.168	0.174	0.177	0.195
60	0.179	0.197	0.209	0.218	0.228	0.247
90	0.195	0.219	0.240	0.250	0.258	0.274
120	0.198	0.227	0.268	0.278	0.291	0.309
150	0.216	0.253	0.290	0.300	0.307	0.329

In Table 5 and Figure 6, a brief cluster building time (CBT) assessment of the EAGTOC-UIVN with recent approaches is given. The result implies that the GA approach failed to represent effectual outcomes with maximal value of CBT. Simultaneously, the EALC, ACO, and GBLADSR techniques attained closer CBT values. Even though the SIC approach tried to demonstrate a reasonable CBT value, the EAGTOC-UIVN technique obtained effectual outcomes with the lowest CBT values. Note that the EAGTOC-UIVN method has attained a minimum CBT value of 0.51 s under 30 nodes.
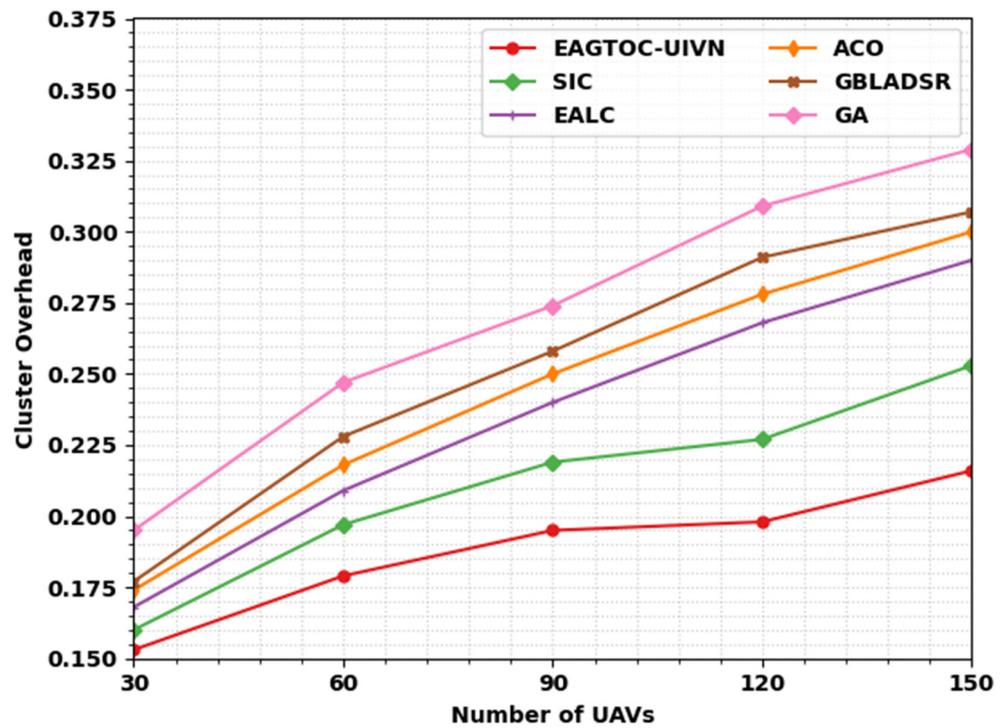
Figure 5. COH analysis of EAGTOC-UIVN algorithm under varying UAVs.

Table 5. CBT analysis of EAGTOC-UIVN technique with other systems under varying nodes.

Cluster Building Time (s)					
Number of Nodes	**EAGTOC-UIVN**	**SIC**	**EALC**	**ACO**	**GBLADSR**	**GA**
30	0.51	2.90	7.87	10.46	14.03	17.41
60	5.29	8.07	12.05	13.44	19.80	30.14
90	5.68	10.46	14.63	21.19	28.15	36.90
120	5.49	10.86	17.02	23.38	39.88	52.01
150	6.08	9.26	19.01	29.74	49.82	60.36

Table 6 and Figure 7 show the cluster average lifetime (CALT) analysis of the EAGTOC-UIVN technique under various nodes. The experimental value implies that the EAGTOC-UIVN approach attained an improved performance under all nodes. For example, on 30 nodes, the EAGTOC-UIVN technique attained an improved CALT value of 67.61 s. On the other hand, the SIC, EALC, ACO, GBLADSR, and GA systems attained minimized CALT values of 66.21 s, 65.20 s, 63.17 s, 54.66 s, and 47.81 s, correspondingly. Meanwhile, on 150 nodes, the EAGTOC-UIVN approach gained an improved CALT value of 55.04 s. In contrast, the SIC, EALC, ACO, GBLADSR, and GA techniques attained reduced CALT values of 50.35 s, 46.03 s, 40.45 s, 37.02 s, and 30.30 s, correspondingly.

Table 7 and Figure 8 show the number of alive nodes (NOAN) investigation of the EAGTOC-UIVN technique under various rounds. The experimental value implies that the EAGTOC-UIVN approach gained improved performance under all rounds. For example, on 400 rounds, the EAGTOC-UIVN system reached an improved NOAN value of 100. In contrast, the SIC, EALC, ACO, GBLADSR, and GA approaches attained reduced NOAN values of 98, 95, 93, 92, and 83, correspondingly. Meanwhile, on 1800 rounds, the EAGTOC-UIVN model gained an improved NOAN value of 71. In contrast, the SIC, EALC, ACO, GBLADSR, and GA methods attained improved NOAN values of 44, 20, 11, 4, and 0, correspondingly.
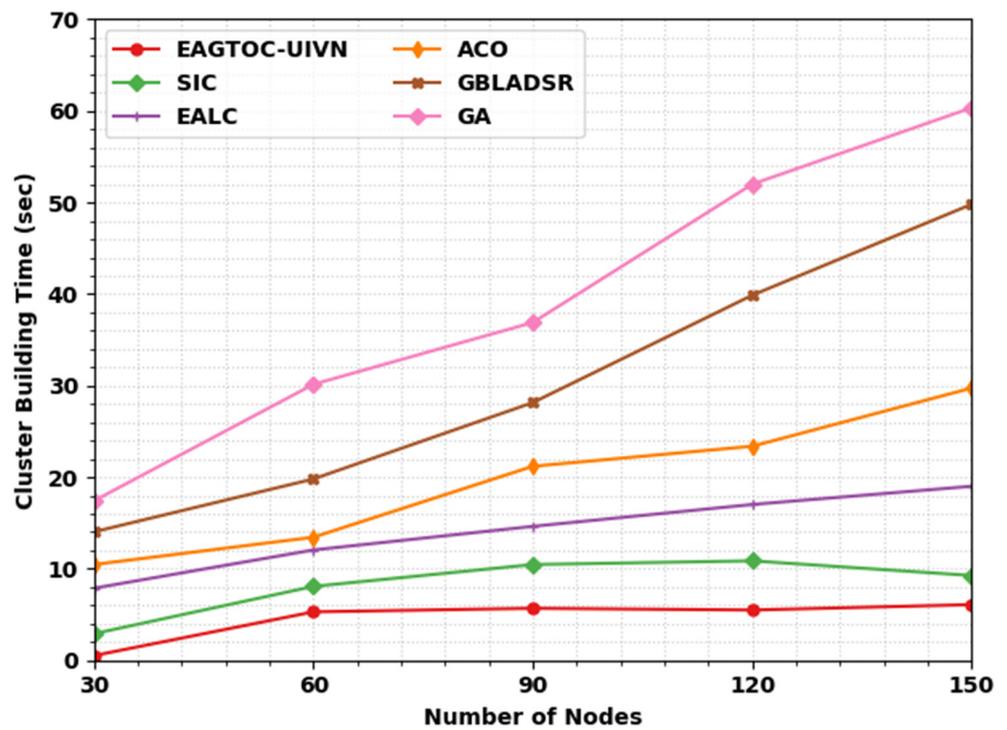
Figure 6. CBT analysis of EAGTOC-UIVN technique under varying nodes.

Table 6. CALT analysis of EAGTOC-UIVN method with other techniques under varying nodes.

Cluster Average Lifetime (s)					
Number of Nodes	**EAGTOC-UIVN**	**SIC**	**EALC**	**ACO**	**GBLADSR**	**GA**
30	67.61	66.21	65.20	63.17	54.66	47.81
60	67.10	64.56	61.14	57.96	48.57	41.59
90	61.77	54.28	53.52	51.24	44.00	34.61
120	58.22	51.24	48.95	46.03	36.01	31.06
150	55.04	50.35	46.03	40.45	37.02	30.30

Table 7. NOAN analysis of EAGTOC-UIVN technique with other systems under varying rounds.

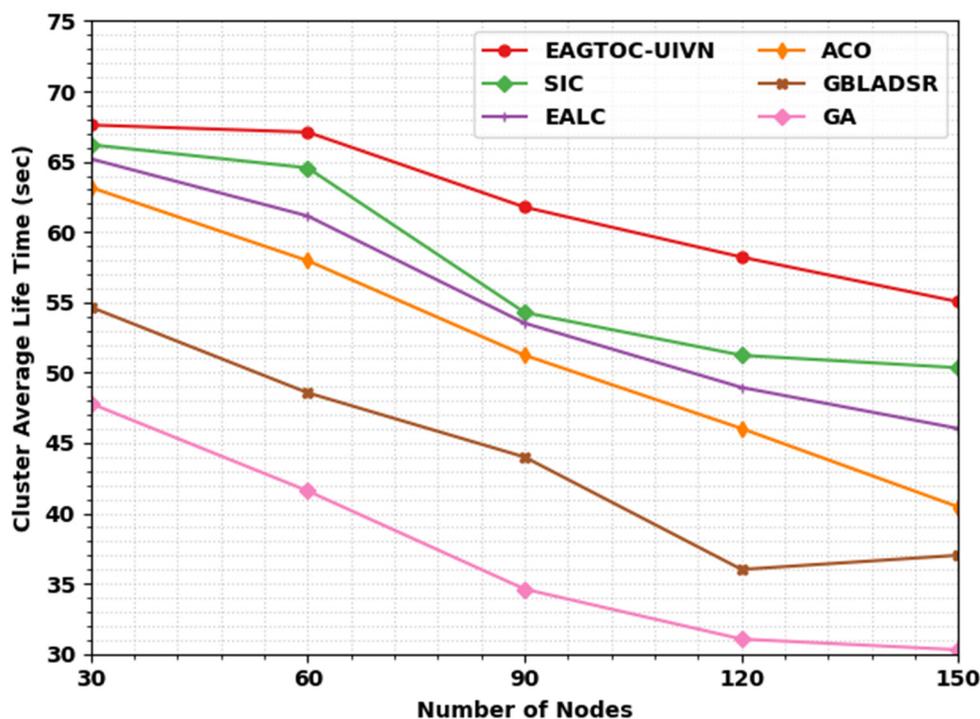| No. of Alive Nodes					
No. of Rounds	**EAGTOC-UIVN**	**SIC**	**EALC**	**ACO**	**GBLADSR**	**GA**
0	100	100	100	100	100	100
200	100	100	99	96	95	92
400	100	98	95	93	92	83
600	99	98	90	85	76	70
800	97	92	88	77	62	61
1000	95	87	83	60	55	51
1200	94	75	68	52	43	30
1400	89	69	59	38	33	15
1600	80	55	45	24	15	3
1800	71	44	20	11	4	0
2000	58	28	9	0	0	0

Figure 7. CALT analysis of EAGTOC-UIVN algorithm under varying nodes.

In Table 8 and Figure 9, a brief total energy consumption (TECON) assessment of the EAGTOC-UIVN technique with recent approaches is given. The outcomes imply that the GA technique has failed to describe effectual outcomes with maximal values of TECON.

Table 8. TECON analysis of EAGTOC-UIVN technique with other systems under varying rounds.

Total Energy Consumption (J)					
No. of Rounds	**EAGTOC-UIVN**	**SIC**	**EALC**	**ACO**	**GBLADSR**	**GA**
0	0.00	0.00	0.00	0.00	0.00	0.00
200	38.61	70.97	80.92	100.84	123.24	247.68
400	98.35	165.55	200.39	225.28	250.17	466.71
600	182.97	265.11	337.29	392.04	441.82	568.76
800	270.09	369.64	476.67	553.83	563.78	643.43
1000	377.11	511.51	578.72	630.98	708.14	718.10
1200	494.09	578.72	660.85	787.79	812.68	790.28
1400	603.61	693.21	770.37	862.46	899.79	884.86
1600	673.30	795.26	867.44	912.24	952.06	937.13
1800	755.43	859.97	917.22	949.57	979.44	976.95
2000	770.37	869.93	947.08	954.55	984.42	996.86

Simultaneously, the EALC, ACO, and GBLADSR techniques obtained closer TECON values. Even though the SIC system tried to show a reasonable TECON value, the EAGTOC-UIVN approach attained effectual outcomes with minimal TECON values. Note that the EAGTOC-UIVN method attained a minimum TECON value of 38.61 J under 200 rounds. From these results, it is evident that the presented model improves the overall network efficacy.
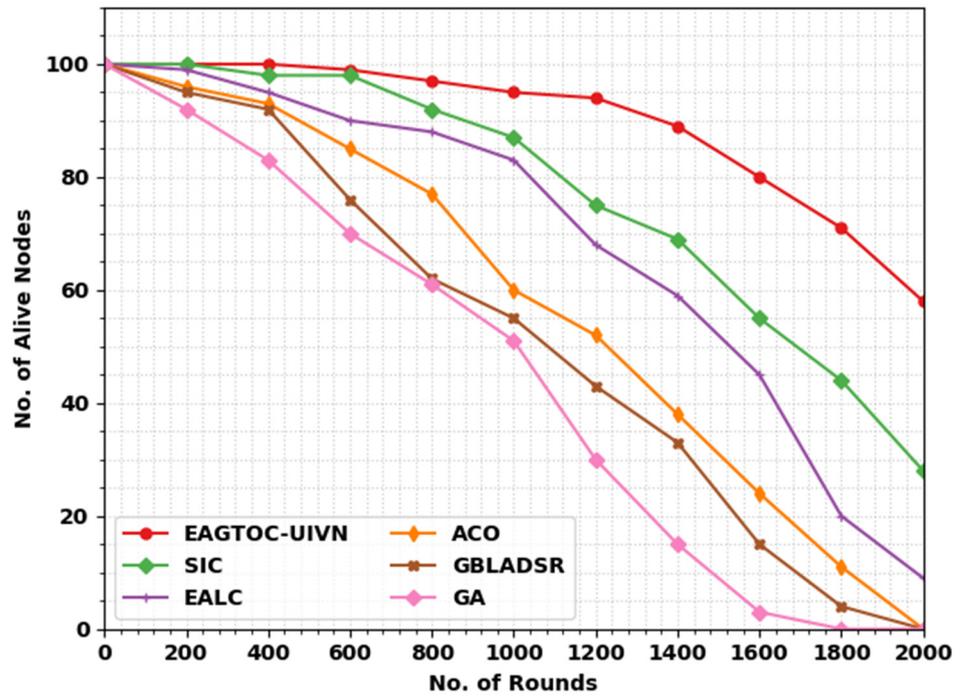
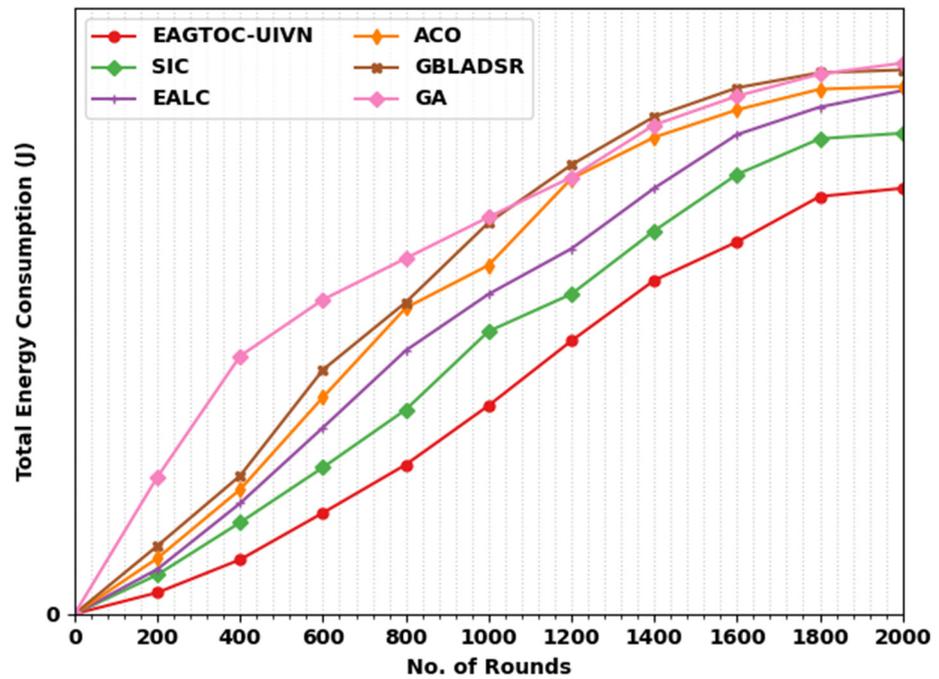**Figure 8.** NOAN analysis of EAGTOC-UIVN algorithm under varying rounds.

Figure 9. TECON analysis of EAGTOC-UIVN algorithm under varying rounds.

5. Conclusions

In this study, a new EAGTOC-UIVN technique was developed for clustering the UAV-assisted VN. The major aim of the EAGTOC-UIVN technique exists in the grouping of the nodes in UAV-based VN to achieve maximum lifetime and energy efficiency. In the presented EAGTOC-UIVN technique, the EAGTO algorithm is primarily designed by the use of the circle chaotic mapping technique. Moreover, the EAGTOC-UIVN technique computes a fitness function with the inclusion of multiple parameters. To depict the improved performance of the EAGTOC-UIVN technique, a widespread simulation analysis

was performed. The comparison study reported the enhancements of the EAGTOC-UIVN technique over other recent approaches. In the future, data aggregation and localization techniques can be designed to increase the overall network effectiveness of the UAV-based VNs.

Conflicts of Interest: The authors declare that they have no conflict of interest. The manuscript was written through contributions of all authors. All authors have given approval to the final version of the manuscript.

References

1. Fatemidokht, H.; Rafsanjani, M.K.; Gupta, B.B.; Hsu, C.H. Efficient and secure routing protocol based on artificial intelligence algorithms with UAV-assisted for vehicular ad hoc networks in intelligent transportation systems. *IEEE Trans. Intell. Transp. Syst.* **2021**, *22*, 4757–4769. [CrossRef]
2. Amantayeva, A.; Yerzhanova, M.; Kizilirmak, R.C. UAV location optimization for UAV-to-vehicle multiple access channel with visible light Communication. In Proceedings of the 2019 Wireless Days (WD), Manchester, UK, 24–26 April 2019; pp. 1–4.
3. Huang, S.; Huang, C.; Wu, D.; Yin, Y.; Ashraf, M.; Fu, B. UAV-Assisted Sensor Data Dissemination in mmWave Vehicular Networks Based on Network Coding. *Wirel. Commun. Mob. Comput.* **2022**, *2022*, 2576182. [CrossRef]
4. Al-Hilo, A.; Samir, M.; Assi, C.; Sharafeddine, S.; Ebrahimi, D. A cooperative approach for content caching and delivery in UAV-assisted vehicular networks. *Veh. Commun.* **2021**, *32*, 100391. [CrossRef]
5. Barka, E.; Kerrache, C.A.; Lagraa, N.; Lakas, A. Behavior-aware UAV-assisted crowd sensing technique for urban vehicular environments. In Proceedings of the 2018 15th IEEE Annual Consumer Communications & Networking Conference (CCNC), Las Vegas, NV, USA, 12–15 January 2018; pp. 1–7.
6. Mokhtari, S.; Nouri, N.; Abouei, J.; Avokh, A.; Plataniotis, K.N. Relaying Data with Joint Optimization of Energy and Delay in Cluster-based UAV-assisted VANETs. *IEEE Int. Things J.* **2022**. [CrossRef]
7. Khabbaz, M.; Antoun, J.; Assi, C. Modeling and performance analysis of UAV-assisted vehicular networks. *IEEE Trans. Veh. Technol.* **2019**, *68*, 8384–8396. [CrossRef]
8. Hu, J.; Chen, C.; Cai, L.; Khosravi, M.R.; Pei, Q.; Wan, S. UAV-assisted vehicular edge computing for the 6G internet of vehicles: Architecture, intelligence, and challenges. *IEEE Commun. Stand. Mag.* **2021**, *5*, 12–18. [CrossRef]
9. Xing, N.; Zong, Q.; Dou, L.; Tian, B.; Wang, Q. A game theoretic approach for mobility prediction clustering in unmanned aerial vehicle networks. *IEEE Trans. Veh. Technol.* **2019**, *68*, 9963–9973. [CrossRef]
10. Fawaz, W. Effect of non-cooperative vehicles on path connectivity in vehicular networks: A theoretical analysis and UAV-based remedy. *Veh. Commun.* **2018**, *11*, 12–19. [CrossRef]
11. Nomikos, N.; Gkonis, P.K.; Bithas, P.S.; Trakadas, P. A Survey on UAV-Aided Maritime Communications: Deployment Considerations, Applications, and Future Challenges. *arXiv* **2022**, arXiv:2209.09605.
12. Wang, H.-M.; Zhang, X.; Jiang, J.-C. UAV-involved wireless physical-layer secure communications: Overview and research directions. *IEEE Wirel. Commun.* **2019**, *26*, 32–39. [CrossRef]
13. Oubbati, O.S.; Chaib, N.; Lakas, A.; Lorenz, P.; Rachedi, A. UAV-assisted supporting services connectivity in urban VANETs. *IEEE Trans. Veh. Technol.* **2019**, *68*, 3944–3951. [CrossRef]
14. Al-Hilo, A.; Samir, M.; Assi, C.; Sharafeddine, S.; Ebrahimi, D. UAV-assisted content delivery in intelligent transportation systems-joint trajectory planning and cache management. *IEEE Trans. Intell. Transp. Syst.* **2020**, *22*, 5155–5167. [CrossRef]

15. He, Y.; Nie, L.; Guo, T.; Kaur, K.; Hassan, M.M.; Yu, K. A NOMA-enabled framework for relay deployment and network optimization in double-layer airborne access VANETs. *IEEE Trans. Intell. Transp. Syst.* **2022**, *23*, 22452–22466. [CrossRef]
16. Khabbaz, M.; Assi, C.; Sharafeddine, S. Multihop V2U Path Availability Analysis in UAV-Assisted Vehicular Networks. *IEEE Int. Things J.* **2021**, *8*, 10745–10754. [CrossRef]
17. Zheng, K.; Sun, Y.; Lin, Z.; Tang, Y. UAV-assisted online video downloading in vehicular networks: A reinforcement learning approach. In Proceedings of the 2020 IEEE 91st Vehicular Technology Conference (VTC2020-Spring), Antwerp, Belgium, 25–28 May2020; pp. 1–5.
18. Raza, A.; Bukhari, S.H.R.; Aadil, F.; Iqbal, Z. An UAV-assisted VANET architecture for intelligent transportation system in smart cities. *Int. J. Distrib. Sens. Netw.* **2021**, *17*, 15501477211031750. [CrossRef]
19. Wu, H.; Lyu, F.; Zhou, C.; Chen, J.; Wang, L.; Shen, X. Optimal UAV caching and trajectory in aerial-assisted vehicular networks: A learning-based approach. *IEEE J. Sel. Areas Commun.* **2020**, *38*, 2783–2797. [CrossRef]
20. Ghazzai, H.; Khattab, A.; Massoud, Y. Mobility and energy aware data routing for UAV-assisted VANETs. In Proceedings of the 2019 IEEE International Conference on Vehicular Electronics and Safety (ICVES), Cairo, Egypt, 4–6 September 2019; pp. 1–6.
21. Huang, S.; Huang, C.; Yin, Y.; Wu, D.; Ashraf, M.W.A.; Fu, B. UAV-assisted data dissemination based on network coding in vehicular networks. *IET Intell. Transp. Syst.* **2022**, *16*, 421–433. [CrossRef]
22. Alioua, A.; Senouci, S.M.; Moussaoui, S.; Sedjelmaci, H.; Messous, M.A. Efficient data processing in software-defined UAV-assisted vehicular networks: A sequential game approach. *Wirel. Pers. Commun.* **2018**, *101*, 2255–2286. [CrossRef]
23. Arafat, M.Y.; Moh, S. Localization and clustering based on swarm intelligence in UAV networks for emergency communications. *IEEE Int. Things J.* **2019**, *6*, 8958–8976. [CrossRef]
24. Mohamed, T.A.; Mustafa, M.K. Adaptive trainer for multi-layer perceptron using artificial gorilla troops optimizer algorithm. *Int. J. Nonlinear Anal. Appl.* **2022**. [CrossRef]
25. Lakshmanna, K.; Subramani, N.; Alotaibi, Y.; Alghamdi, S.; Khalafand, O.I.; Nanda, A.K. Improved metaheuristic-driven energy-aware cluster-based routing scheme for IoT-assisted wireless sensor networks. *Sustainability* **2022**, *14*, 7712. [CrossRef]